Atom Indonesia

Journal homepage: https://atomindonesia.brin.go.id

Non-Dimensional Number Analysis on Natural Circulation Flow Changes Inside Straight-Pipe Heat Exchanger of Water Cooling Tank in FASSIP-02 Test Loop

E. P. Ariesta[1], Deendarlianto[1], A. S. Al Amin[1], P. H. Setiawan[2], H. A. Gunawan[2], M. Juarsa[2*]

[1]*Department of Mechanical and Industrial Engineering, Faculty of Engineering, Gadjah Mada University, Jl. Grafika No.2, Yogyakarta 55281, Indonesia*
[2]*Research Center for Nuclear Reactor Technology, National Research and Innovation Agency (BRIN), Tangerang Selatan 15310, Indonesia*

ARTICLE INFO

Article history:
Received 8 November 2023
Received in revised form 3 April 2024
Accepted 21 April 2024

Keywords:
FASSIP-02
Non-dimensional
Straight-pipe
Natural circulation
Passive safety

ABSTRACT

The FASSIP-02 test loop is a large-scale experimental facility that investigates natural circulation flow rate phenomena to improve passive safety systems of nuclear reactors. Heat transfer in the piping system will result in pattern and magnitude of the natural circulation flow being formed, so it is essential to investigate the heat dissipation capabilities, which will later be applied in nuclear passive cooling systems. The heat transfer behavior of passive cooling systems in large-scale facilities can be quantified with non-dimensional numbers. This research analyzes heat transfer in a straight heat exchanger by comparing non-dimensional numbers based on the Dittus-Boetler and McAdams correlation with the correlation generated from experimental data. The analysis results show that the predicted McAdams correlation with the experimental correlation is higher than 83 %. Meanwhile, Dittus Boetler's correlation prediction with the experimental correlation is smaller than 71 %. The dominance of momentum diffusivity in the cooling process shows the characteristics of thermal behavior with the Prandtl number. In addition, all-natural circulation flow variations occur in a turbulent flow regime that increases with increasing water temperature in the heating tank.

INTRODUCTION

The development of safety system technology in nuclear power plants is a concern for researchers to realize the use of nuclear energy to fulfill increasing energy needs. The development of a nuclear reactor safety system is based on the anticipation of accidents caused by natural disasters, such as those in Fukushima Daiichi, Japan the 9.1 M earthquake caused a tsunami that submerged the active cooling system in Fukushima Daiichi, resulted in the failure of residual heat removal during the occurrence of the Station Black Out (SBO). This results in a release of radiation into the environment [1].

Based on the paragraph above, researchers are developing a reactor cooling system using a passive approach to replace the active system coolant during normal operation and accident conditions. The passive cooling system utilizes the phenomenon of natural circulation due to the buoyancy force caused by changes in fluid density based on temperature rise, moving towards parts with lower temperatures so that the fluid density increases, causing gravitational force [2,3]. Based on these two forces, it produces a flow in the fluid that carries heat to the coolant repeatedly. This phenomenon can be applied to the nuclear power plant (NPP) cooling system, removing heat from the heat source to areas with lower temperatures throughout the cooling process [4]. Natural circulation can remove decay

*Corresponding author.
E-mail address: mulya.juarsa@brin.go.id
DOI: https://doi.org/10.55981/aij.2024.1387

heat if the forced circulation failed to work, and natural circulation is widely applied as a secondary reactor cooling system [5]. The direction flow of natural circulation in the passive cooling system depends on certain conditions.

Natural circulation cooling system for NPPs uses pools with large volumes of fluid to remove more heat during an accident [6]. The natural circulation is considered to be used for nuclear safety system power plant for normal operation condition and emergency condition [7]. By using C-shape heat exchangers for heat transfer, in experiments conducted by Daogang et al. (2016) with a multiple heat exchange pipes in the IRWST facility, it was shown that the residual heat distributed to IRWST was continuously stable and the temperature gradient affected the speed of temperature distribution. Still, the heat transfer in C-shape passive residual heat removal heat exchanger (PRHR HX) with a vertical cross-section is better than the horizontal cross-section [8].

Increasing the natural circulation flow in the reactor cooling system can improve heat absorption at the heat source and heat removal from the cooling pool. Research conducted by Ahn et al. (2018) investigating the heat transfer of the U-tube bundle of the cooling tank from the PASCAL and APR+ facilities showed a deviation in the change in heat capacity by 1 % and for the heat transfer coefficient by 2 % based on the difference in diameter size [9]. The temperature distribution that occurs in the C-shape heat exchanger shows that the stratification of the temperature direction tends toward the top of the pool surface outside the heat exchanger pipe [10]. The effect of temperature distribution on heat transfer will have a destructive impact if the temperature distribution is uneven, so that the heat transfer ability decreases [11]. Physically, the temperature decrease of 60 % in the C-shape pipe heat exchanger occurs in the lower horizontal part after heat transfer along the vertical part of the C-shape pipe heat exchanger [12]. Temperature stratification along the vertical side where the upper horizontal part is stunned so that constant heat transfer will increase the temperature of the water in the pool [13]. The increased heat transfer in the cooling pool from the heat exchanger also influences the volume water of cooling pool water. When the heat transfer occurs from the heat exchanger to the pool, it causes a reduction in the volume of water due to evaporation that affects its thermal behavior [14].

The heat transfer ability of C-shape PRHR HX is determined by the dominance of heat transfer, which occurs through convection and conduction. Research related to analysis to determine the dominance of heat transfer was carried out by many researchers, both experimental, dynamic fluid simulation and numerical methods, as well as many developments based on several parameters. Many developments in the science that explain the dominance of heat transfer as shown in Table 1.

Table 1. Nusselt number equation.

Author/ year	Equation	Reference
Dittus-Boelter (1930)	$Nu = 0.023\,Re^{0.8}\,Pr^{n}$ Coefficient of n for heating 0.4 and for cooling 0.3.	[15,16]
Mc Adams (1942)	$Nu = 0.53\,Re^{0.8}\,Pr^{0.4}$ To describe heat transfer High pressures and low heat fluxes.	[15-17]
Krasnochekov and Protopopov (1959)	$Nu_b = Nu_{0,b}\left(\frac{C_P}{C_{p,b}}\right)^{0.35}\left(\frac{k_b}{k_w}\right)^{-0.33}\left(\frac{\mu_b}{\mu_w}\right)^{0.11}$ $Nu_{0,b} = \left(\frac{\frac{f_b}{8}Re_b\,Pr}{12.7\left(\frac{f_b}{8}\right)^{0.5}\left(Pr^{\frac{2}{3}}-1\right)+1.07}\right)$ $f = (1.82\,log_{10}\,(Re_b) - 1.64)^{-2}$	[16,18]
Churchill and Chu (1975)	$Nu = \left(0.825 + \frac{0.387Ra^{1/6}}{(1+(0.437/Pr)^{9/16})^{8/27}}\right)^2$ For natural convection on laminar flow with valid range of Gr . Pr > 10^{-1}.	[19,20]
Gnielinski (1976)	$Nu = \frac{\left(\frac{f}{8}\right)(Re-1000)Pr}{1+12.7\left(\frac{f}{8}\right)^{0.5}\left(Pr^{\frac{2}{3}}-1\right)}$ $f = (0.79\,lnRe - 1.64)^{-2}$ For smooth tube and range Re_N : 10^4 < Re < 10^6.	[18,21]
Jackson and Hall, (1979)	$Nu_b = 0.0183\,Re_b^{0.82}\,Pr^{0.5}\left(\frac{\rho_w}{\rho_b}\right)^{0.3}\left(\frac{C_p}{C_{pb}}\right)^{n}$ $C_p = \left(\int_{Tw}^{Tb} C_p dT\right)/(T_b - T_w)$ n for $T_b<T_w<T_{pc}$ and $1.2T_{pc}<T_b<T_w$ is 0.4 n for $T_b<T_{pc}<T_w$ is $0.4+0.2[(T_w/T_{pc})-1]$ n for $T_{pc}<T_b<1.2T_{pc}$ and $T_b<T_w$ is $0.4+0.2[(T_w/T_{pc})-1][1-5(T_b/T_{pc}-1)]$	[16,18]
Petukhov *et al.*, (1983)	$Nu = \frac{\left(\frac{f}{8}\right)Re_b\,Pr_b}{1+900/Re_b+12.7\left(\frac{f}{8}\right)^{0.5}\left(Pr_b^{2/3}-1\right)}$ $f = f_0(\rho_w/\rho_b)^{0.4}\left(C_p/C_{p,b}\right)^{0.2}$ $f_0 = (1.82\,log\,(Re_b) - 1.64)^{-2}$ Including physical parameter such skin friction of material pipe.	[18,22]
Razumovskiy *et al.*, (1990)	$Nu = \frac{(f_r)\,Re_b\,Pr_b}{1.07+12.7\left(\frac{f}{8}\right)^{0.5}\left(Pr_b^{2/3}-1\right)}\left(\frac{C_p}{C_{p,b}}\right)^{0.65}$ $f_r = f_0(\rho_w/\rho_b)^{0.18}(\mu_w/\mu_b)^{0.18}$	[18]
Kang and Chang (2009)	$Nu_b = 0.0244\,Re_b^{0.765}\,Pr^{0.552}\left(\frac{\rho_w}{\rho_b}\right)^{0.0293}$	[23]
Mokry *et al.* (2010)	$Nu_b = 0.0061\,Re_b^{0.904}\,Pr^{0.833}\left(\frac{\rho_w}{\rho_b}\right)^{0.564}$	[16,18]

Based on Table 1 concerning the study of the dominance of heat transfer in a fluid through a heat exchanger pipe, there is a research development such as that conducted by Dittus-Boelter in 1930, where in describing the dominance of heat transfer that occurs in turbulent flow in a channel where there is heat transfer between the meeting of fluid flow with the channel wall, an increase in fluid temperature in the flow causes a decrease in viscosity. It can be described by the relation of Reynolds numbers for the interpretation of the flow regime that occurs and molecular diffusion due to thermal or momentum of flow motion shown in Eq. (11) [24]. The obstructed flow caused by the material property with different material frictional forces resulted that the equation built by Dittus-Boelter was added by friction parameters on the walls through which the flow passes. It was developed by Krasnochekov and Protopopov in 1959, whom added friction parameters which are functions of Reynolds numbers [18]. The heat transfer capability in heat exchangers for passive cooling systems needs to be analyzed in terms of the dominance of heat transfer that occurs based on the type of flow and the dominance of heat transfer that affects the flow rate.

The Nuclear Reactor Thermal-fluids System research group in the Research Center for Nuclear Reactor Technology, Research Organization for Nuclear Energy - National Research and Innovation Agency (ORTN-BRIN), has built a passive safety system facility called FASSIP-02 Test Loop to investigate flow changes in natural circulation phenomena [25]. The FASSIP-02 Test Loop is a large-scale experimental facility consisting of two significant components, namely the Water Heating Tank (WHT), which functions to provide heat to water, and the Water-Cooling Tank (WCT), which works to remove heat to the environment [26]. A study on heat transfer analysis with height difference in cooling process by Juarsa et al. (2018) showed that the heat removed from water into tube wall was dominated by convection, then heat transfer along the tube thickness was dominated by conduction and heat was released to the outer wall [27]. Analysis of the heat transfer of water flow in pipes is fundamental in developing natural circulation performance for applying passive safety systems to improve nuclear reactor safety, operational conditions, and accidents involving thermals. In addition, differences in elevation orientation of the heat source and cooling section can affect heat transfer in passive cooling systems; there is a friction factor of working fluid with surface roughness in pipes, so the Dittus-Boelter correlation is a mathematical approach method based on the ratio of dimensionless numbers for the case of the relationship of natural convection flow with thermal conductivity [28].

Several researchers conducted research related to the FASSIP-02 Test Loop facility. Juarsa et al. in 2018 calculated natural circulation flow estimates based on temperature on the FASSIP-02 Test Loop, which shows that the magnitude of the temperature difference between WHT and WCT causes a high velocity of fluid flow in the loop [29]. Shevaladze et al. in 2022 showed that temperature difference affected flow change in cooling tank, where the released heat increasing the temperature difference [30]. The fluid flow character of the FASSIP-02 Test Loop in the WCT section is essential in predicting heat transfer through natural circulation to the influence of viscosity, thermal conductivity, and such as determining the ratio between convection in water in loops to the conduction of pipes passed by water based on thermal treatment on the walls of the heat exchanger pipe in WCT so that the flow of water in the pipe can work aerodynamics with a mathematical approach. The mathematical calculation approach to the analysis of dimensionless numbers to compare natural circulation flows to parameters that affect the flow can be defined in the correlation formed by Dittus-Boelter, where correlation can determine the heat convection coefficient with the relationship of functions to Reynolds numbers and Prandtl numbers.

Prandtl and Reynolds numbers can be obtained from heat transfer that occurs in fluid flow in heat exchanger pipes using the Dittus-Boelter correlation method to increase the efficiency of the heat transfer system in WCT. This research aims to determine the magnitude and characteristics of heat transfer in a C-shaped straight pipe heat exchanger inside a water cooling tank based on changes in water temperature inside the heating tank. Quantitative indicators are shown by the relationship of the Nusselt number as a function of changes in the Reynolds and Prandt numbers. The results of fitting non-domestic number correlations from experimental data on large-scale passive cooling facilities were analyzed by comparing them with the correlations from other studies. So, a non-dimensional number map is obtained as the relationships between the Nusselt, Reynold, and Prandt numbers from experimental data with other similar correlations.

NON-DIMENSIONAL NUMBER IN NATURAL CIRCULATION FLOW

Reynold's numbers in this experiment aim to show the flow regime that occurs in a pipe or loop, where the flow regime value can be determined by the range for laminar flows from 2000 to 3000, for transition flows from 3000 to 4000, and for turbulent flows Re≥ 4000 [31]. Reynolds numbers can be global and local depending on scaling. In a global definition, it shows the overall constraints of the problem boundary, while locally, it indicates the state of the shear layer [32]. The flow regime in this experiment influences temperature changes that occur in inlet and outlet heat exchangers in WCT without forced convection, where water viscosity does not block the kinetic energy in water to thermal behavior. Using calculations with Reynold numbers can describe the effect of the regime flow based on differential temperature with Reynold (Re) number values expressed in Eq. (1).

$$\mathrm{Re} = \frac{\rho v D}{\mu} \tag{1}$$

where ρ is density of fluid as a function of temperature (kg/m^3), v velocity of fluid obtained from flowrate data (m/s). Loop pipe diameter D (in m) affected fluid velocity, and viscosity of the fluid (μ) as a function of temperature (kg/m.s). Density and viscosity in this study use correlation of temperature function. The Reynolds number's density parameter is a temperature function and determined using Eq. (2).

$$\rho = \begin{pmatrix} 1004.78904 - 0.046283T_F \\ -7.9738 \times 10^{-4} T_F^2 \end{pmatrix} \tag{2}$$

where $T_F = 1.8T + T$, T is average between temperature inside WCT and temperature outside of WCT. The viscosity in Reynolds's number is determined by an equation that uses temperature as a viscosity function, shown in Eq. (3).

$$\mu = \exp\left(\frac{-6.32520396+(-0.0888323T)}{1+(8.765317\times10^{-3})T+(-9.657\times10^{7}T^{2})}\right) \tag{3}$$

where T is the temperature in the equation to determine dynamic viscosity (Pa.s). The temperature used in Eq. (1), Eq. (2), and Eq. (3) is the average temperature between the temperature inside and outside of WCT. In addition to obtaining a flow regime on the FASSIP-02 Test Loop with Reynolds' numbers, a ratio of momentum diffusivity or kinematic viscosity of thermal diffusivity of water in a heat exchanger pipe in WCT can be obtained by Prandtl number analysis. The Prandtl number on the turbulent flow can be used to calculate the contribution of energy transfer while the heat displacement of the fluid is always constant and the value is close to one [33]. Thus, Eq. (4) is obtained.

$$\mathrm{Pr} = \frac{\mu\, Cp}{K} \tag{4}$$

Based on the simplification of Eq. (4), three parameters determine the magnitude of the value of other parts of the fluid viscosity and specific heat of the water, that is inversely proportional to its thermal conductivity (W/m.K). The importance of the water viscosity in the Prandtl number equation is used in Eq. (3), which is a function of temperature. In contrast, the heat specific (Cp) calorific value of water and the thermal conductivity (k) of water as a function of the temperature was obtained based on Eq. (5) and Eq. (6).

$$Cp = \sqrt{\frac{17.48508904+(-0.0318959917T)}{1+(=1.6750\times10^{-3}T)+(5.66294725\times10^{-9}T^{3})}} \tag{5}$$

Based on Eq. (5) in determining the specific heat of water (J/kg.K), a functional equation was used to determine the average temperature of the water entering the WCT (TC_{in}) and exiting (TC_{out}). The value of water conductivity present in the WCT heat exchanger can be obtained by Eq. (6).

$$k = 0.5677829144 + 1.877417 \times 10^{-3}T \\ (8.17790 \times 10^{-6}T^2) + (5.66294725 \times 10^{-9}T^3) \tag{6}$$

After obtaining the parameters in Eq. (1) and Eq. (4), the analysis of the Prandtl numbers and the Reynolds' numbers can be carried out by a study of the Nusselt numbers, which are the equations of the Reynolds number function (Re) and the Prandtl number (Pr), where the correlation formed based on the two non-dimensional numbers so that the correlation obtained is based on experimental data. Finally, the application of Nusselt numbers with Reynolds number functions and Prandtl numbers applied in Gnielinski correlation to cooling processes at WCT is expressed in Eq. (7) [21].

$$Nu = \frac{\left(\frac{f}{8}\right)(\mathrm{Re}-1000)\mathrm{Pr}}{1+12.7\left(\frac{f}{8}\right)^{0.5}\left(\mathrm{Pr}^{2/3}-1\right)} \tag{7}$$

The obtained Gnielinski correlation has a validation of the Prandtl number range of $0.5 \leq \mathrm{Pr} \leq 2000$ and the proof of the Reynolds number range of $3000 \leq \mathrm{Re} \leq 5 \times 10^6$. Based on Eq. (7), f is a dimensionless quantity used in the Darcy-Weisbach equation to describe the friction factor of flow in a

pipe, so it is expressed in the Reynolds number function in as in Eq. (8).

$$f = (0.79 \ln \mathrm{Re} - 1.64)^{-2} \quad (8)$$

Equation 8 describes Darcy-Weisbach friction factor which involve the result of Reynolds number from Eq. (1). The analysis process was carried out by mathematical approach using Microsoft Excel software to obtain new correlations using equations with an approach of experimental data fitting through graphical software. The correlation of Nusselt numbers in heat exchangers in WCT can be constructed based on the relationship function between Reynolds' number and the Prandtl number, by using the Dittus-Boelter equation expressed as follows.

$$\left(\frac{hD}{k}\right) = 19.5 \left(\frac{Dv}{\mu}\right)^{0.8} \left(\frac{Cp\,\mu}{k}\right)^{n} \quad (9)$$

Based on Eq. (9), it is known that *h* is the convection coefficient (J/m^2.K) were to define heat transfer coefficient convection, *D* is the cross-sectional diameter of the flow (m), *k* is the conduction coefficient (J/m.K), μ is dynamics viscosity (Pa.s), *v* is the flow velocity (m/s), and C_p is specific heat (J/kg.K) while for the value of *n* for heating conditions is 0.4 and for cooling requirements is 0.3 [34]. Based on the correlation shown in Eq. (9), it can be simplified to Eq. (10).

$$Nu = 0.023\ \mathrm{Re}^{0.8}\mathrm{Pr}^{0.4} \quad (10)$$

So that a general form of the Dittus-Boelter correlation can be obtained, which is used to analyze the heat transfer in the flow and related to Nusselt number, so that it is expressed in Eq. (11).

$$Nu = C\ \mathrm{Re}^{\mathrm{m}}\mathrm{Pr}^{\mathrm{n}} \quad (11)$$

The *C* constant in Eq. (11) is obtained based on the McAdams correlation, where the friction factor is $S_t = f/8$ with *f* is 0.184 Re-0.2 [15]. There are methods and steps taken to get experimental data so that analysis can be carried out. The following are the methods carried out in conducting experiments, ranging from experimental facilities, measuring and data acquisition, determining the testing matrix, setup control in experiments, and procedures in processing experimental data.

EXPERIMENT METHODOLOGY

The experiment was carried out by applying thermal treatment to the water in WHT using four heating elements with a heating element power of 5 kW each with temperature variations setting of 40 °C, 50 °C, 60 °C, 70 °C, and 80 °C.

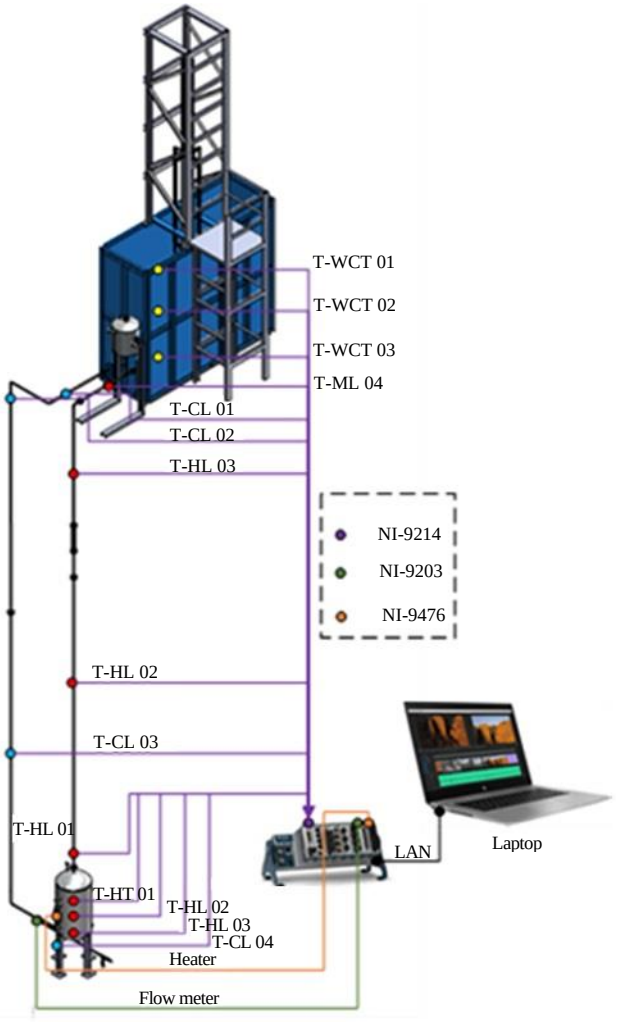

Fig. 1. Acquisition and control system.

Initial condition data was recorded using the National Instrument (NI) module to record temperature data and flow rate, and to control the heating element. The data acquisition and control scheme in the FASSIP-02 Test Loop experiment is shown in Fig. 1. Based on Fig. 1, the acquisition data obtained is the temperature data recorded by NI-9214 and the water discharge data in the loop through the flow meter that flows out the current output, which is then converted into discharge data with the NI-9203 module. The heating element control system that will provide power input is set with the NI-9476 module with the scenarios shown in the matrix table in Table 2.

Table 2. Experiment matrix.

Material loop	Heat exchanger tipe inside WCT	Temperature variation
SS 304 (1 inch)	*Straight Tube*	40 °C
		50 °C
		60 °C
		70 °C
		80 °C

Based on Table 2, experiments were carried out by providing power to the heater in WHT to increase the water temperature until it reaches the average water temperature, in order to increase temperature variations in the experimental matrix. The condition when the water temperature is increased is transient in the experiment, and after reaching the intended temperature, it will be maintained for 5 hours. In the experiment, several heaters continue to supply power to the heater, as shown in Table 3 for heating schemes in steady state condition.

Table 3. Steady state heating.

Temperature Variation	Steady State $T_{set} \leq T_{act}$			
	H1	H2	H3	H4
40 ºC	ON/OFF	ON/OFF	OFF	OFF
50 ºC	ON/OFF	ON/OFF	OFF	OFF
60 ºC	ON/OFF	ON/OFF	OFF	OFF
70 ºC	ON/OFF	ON/OFF	ON/OFF	OFF
80 ºC	ON/OFF	ON/OFF	ON/OFF	ON/OFF

Table 3 shows the scenario for water inside the WHT to be heated up using four heaters, with each heater controlled using the NI-9476 module via a solid-state relay (SSR). To increase the water temperature until it reached the initial setting temperature of 40 ºC, 50 ºC, 60 ºC, 70 ºC, and 80 ºC, all heaters (H1, H2, H3, and H4) were used. In case to maintain the steady-state condition for setting temperatures of 40 ºC, 50 ºC, and 60 ºC, two heaters (H1 and H2) are set to be ON/OFF using SSR, and another two heaters (H3 and H4) are set to be OFF. Meanwhile, to maintain the steady state of setting a temperature of 70 ºC, three heaters (H1, H2, and H3) are set to be ON/OFF using SSR, and one heater (H4) is set to be OFF. For water setting temperature of 80 ºC, all heaters (H1, H2, H3, and H4) were controlled to be ON/OFF condition. Data acquisition and control in experiments are carried out using the LabVIEW program. The data will be displayed in the form of graphs for analysis using Origin 8 and Microsoft Excel for calculations, to obtain the results.

RESULTS AND DISCUSSION

Based on the results of experimental data, characterization of the average temperature of water in WHT, inlet temperature, and WCT outlets and average water temperature in WCT for each temperature variation is shown in Figs. (2-4).

Figure 2 shows the results of the characterization of WHT average water temperature to thermal treatment by providing heat through heating elements, controlled by Solid State Relay (SSR). The experimental temperature variations caused time differences in increasing water temperature in WHT. The time required to achieve temperature variations of 40 °C, 50 °C, 60 °C, 70 °C, and 80 °C respectively takes 1314 seconds, 2508 seconds, 3683 seconds, 4332 seconds, and 6820 seconds, with the maximum average temperature in WHT are 40 °C, 44 °C, 53 °C, 61 °C, and 70 °C. Based on Fig. 2, temperature variation of 40 ºC encounters fluctuations due to the small amount of heat received by the strand into the WHT and the result of the release of heat into the water in the WTC, causing a rapid decrease in temperature. In contrast, the amount of heat from the heater in the WHT was still being supplied, and the condition occurred repeatedly. Temperature characterization in the FASSIP-02 Test Loop shows a temperature difference between the WHT and WCT parts, causing a change in mass flow at each variation in water saturation temperature, as shown in Fig. 3.

Figure 3 shows the recording results of the average water temperature in WCT, ranging from transient heating and steady-state to cooling transient conditions. The maximum temperature achieved at the WHT temperature variation of 40 °C, 50 °C, 60 °C, 70 °C, and 80 °C are 38 °C, 45.22 °C, 53 °C, 62.45 °C, and 70.45 °C. The temperature difference between WHT and WCT occurs as shown below.

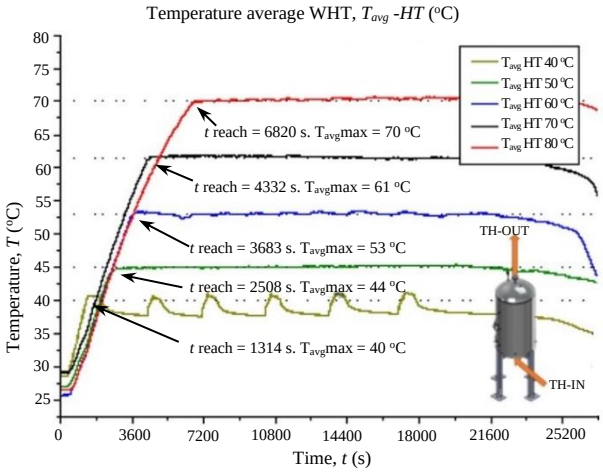

Fig. 2 Measurement of average temperature in WHT.

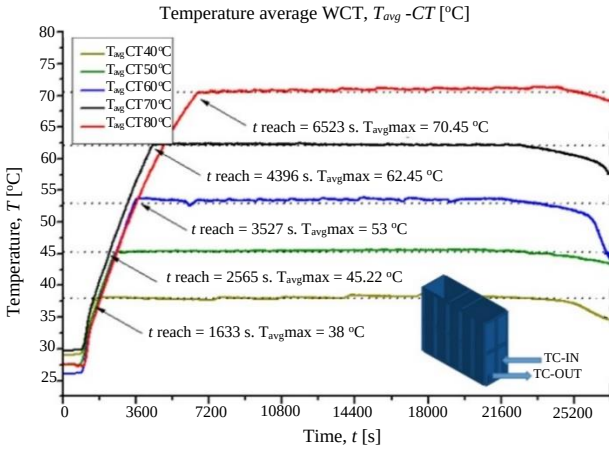

Fig. 3 Measurement average temperature WCT.

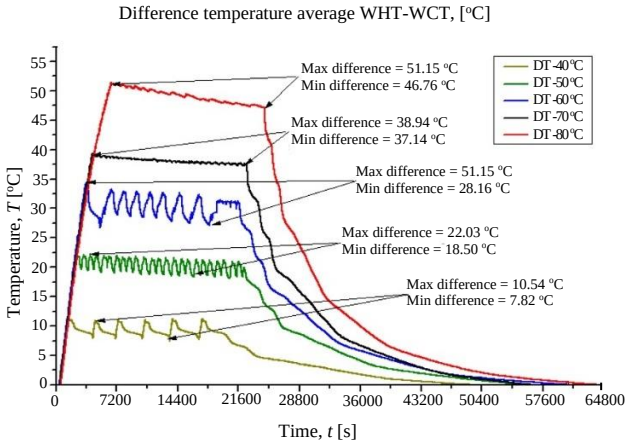

Fig. 4. Difference Temperature between WHT and WCT.

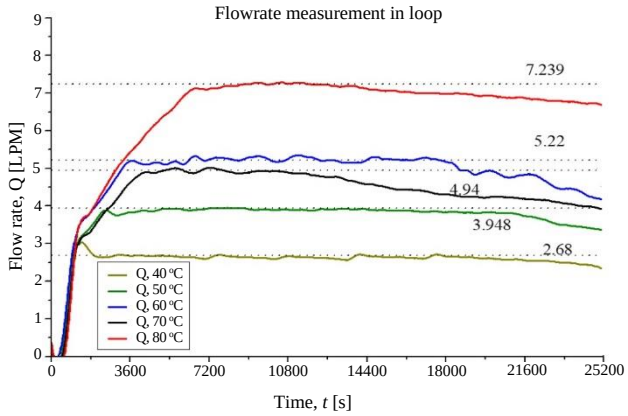

Fig. 5 Flow rate measurement.

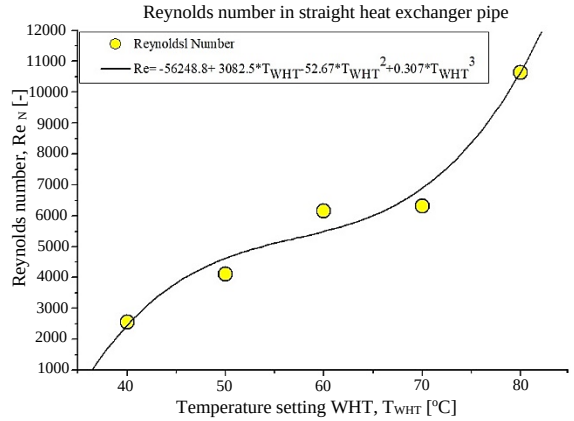

Fig. 6 Analysis of reynolds number.

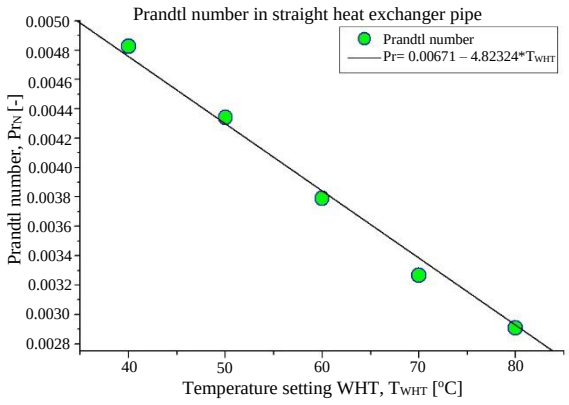

Fig. 7 Analysis of prandtl number.

Figure 4 shows the difference in temperature variation 40 °C, 50 °C, 60 °C, 70 °C, and 80 °C. For example, a temperature variation 80 °C shows a maximum difference of 51.15 °C and a minimum difference of 46.76 °C. Still, in temperature of 70 °C, there is a slight maximum and minimum difference, so there is a decrease in flow rate compared to temperature variation 60 °C, which has a vast difference in maximum and minimum temperatures in Fig. 5. The flow rate is greater than the temperature of 70 °C.

The size of the natural circulation flow in the experiment temperatures 40 °C, 50 °C, 60 °C, 70 °C, and 80 °C based on Fig. 5 shows that the size of the natural circulation flow at a 80 °C is the most significant, reaching 7.239 LPM, and the least significant flow at a temperature variation of 40 °C of 2.68 LPM. The Fig. 5 shows a substantial increase in flow rate measurement results at temperature variations of 40 °C, 50 °C, 60 °C, 70 °C and 80 °C.

The magnitude of the flow value in the heat exchanger in WCT affects the flow regime at different temperatures on Reynolds numbers. Based on Eq. (1), for each experimental temperature variation, the magnitude of the the Reynolds number in the heat exchanger in the WCT was obtained, as shown in Fig. 6.

Figure 6 shows the transient to the steady-state condition of the Reynolds numbers in the U-shape heat exchanger pipe. In the steady-state condition, the average of the Reynolds numbers with temperature range of 40 °C to 80 °C in the laminar regime to a turbulent regime is 2554 to 10640.

Increased temperature in the WHT decreased viscosity of the water. Analysis of Prandtl numbers, the ratio of thermal diffusivity and kinematic viscosity in heat exchangers in WCT are shown in Fig. 7.

Figure 7 shows the magnitude of the Prandtl number based on the increase in temperature. The Prandtl number decreases when heated. It is caused by the decrease in viscosity proportional to the magnitude of its thermal conductivity. This is seen between temperature range of 50 °C to 80 °C, with the obtained Prandtl numbers of 0.00434 and 0.00291, respectively. Figure 8 shows the relationship between the average of the Nusselt number divided by the Prandtl number versus the Reynolds number as flow regime variables for steady state conditions obtained at each variation of water temperature settings from 40 °C to 50 °C, 60 °C, and 80 °C.

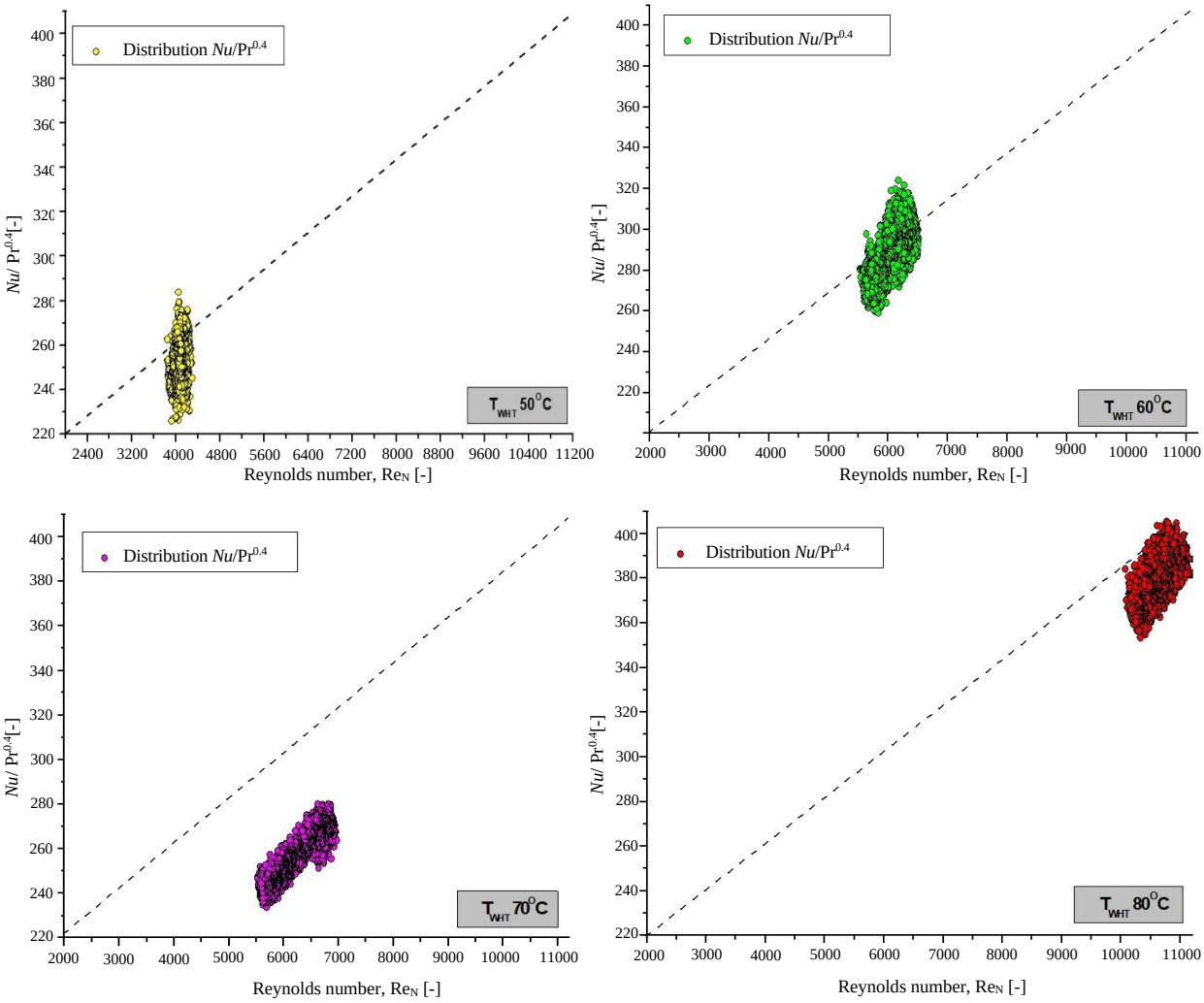

Fig. 8 Nusselt number distribution with T_{WHT} variation.

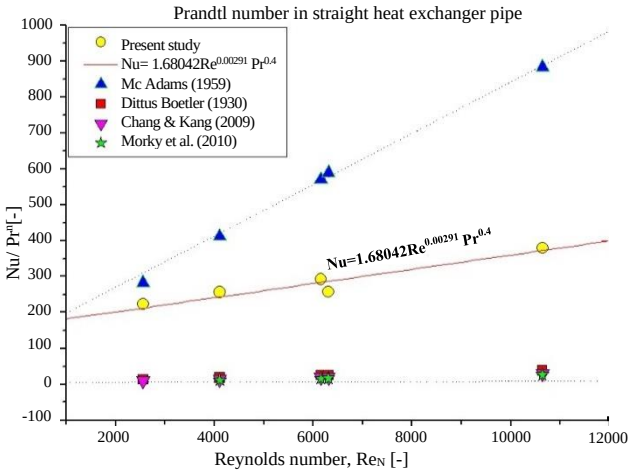

Fig. 9 Comparation nusselt number with other research.

Based on Fig. 8, the distribution of Nusselt numbers along the temperature variations shows that the increase in temperature variation is inversely proportional to the magnitude of the Nusselt number. This is caused by the rise in temperature, causing a decrease in the convective heat transfer coefficient. Therefore, the heat transfer coefficient dominates from heat transfer in the heat exchanger in WCT as seen between temperature variations 50 °C and 80 °C, with the resulting Nusselt numbers of 1.13 and 0.48, respectively. Temperature of 70 °C shows a decrease caused by temperature difference in WHT and WCT. Although only 1.8 °C, it affected the flowrate in the straight heat exchanger pipe. It also affected Reynolds number, but in this variation, the flow regime is turbulent. Nusselt number in the heat exchanger distribution compared to other research for as function of Reynolds number and Prandtl number is shown in Fig. 9.

As a result, natural convection heat transfer correlates Nusselt's number with the experiment data. Comparing the present study may not fit with other research, with the McAdams correlation shown over the predicted value of the present study and the Dittus-Boetler correlation being less predicted than experimental data. Correlation Dittus-Boetler, Chang & Kang, and Morky et al. showed good agreement with experimental data. Correlation from experimental data obtained by fitting linear shown in Eq. (12).

$$Nu = 1.68042\mathrm{Re}^{0.0198}\mathrm{Pr}^{0.4} \quad (12)$$

According to Fig. 9, the predicted McAdams correlation with the experimental correlation is larger than 83 %. Meanwhile, Dittus Boetler's correlation prediction with the experimental correlation is less than 71 %. This study's correlation has different characteristics from the correlation of several researchers due to the use of a straight pipe heat exchanger in the WCT. Besides, the main factor is that the size of the FASSIP-02 test loop experimental facility is larger than the geometry used by other researchers.

CONCLUSION

The characteristics of the average temperature in WHT show variations in temperatures of 40 °C, 50 °C, and 60 °C. There is a decrease temperature due to residual heat of about 2.5 ^{o}C. Characterization of the average temperature in WCT shows the variation in temperature 40 °C. The measured temperature is lower than the variation of 80 °C by 38 ^{o}C, while at a temperature of 80 ^{o}C measured in WCT is 29.5 ^{o}C.

The temperature difference between WHT and WCT obtained natural circulation flow at a temperature variation of 80 °C of 7,239 LPM and the lowest at a temperature of 40 °C with a flow rate of 2.68 LPM. Reynolds number analysis of temperature variations of 40 °C up to 80 ^{o}C showed a flow regime ranging from 2554 to 10640.

The distribution of the Nusselt number, according to Fig. 7, shows a decreasing value at 70 °C, which caused a difference in temperature in WHT and WCT of only 1.8 °C. The magnitude of the Prandtl number at a temperature variation of 40 °C to 80 °C is 0.00434 and 0.00291. Nusselt number relation in WCT based on Dittus-Boelter method from experimental data with a C constant of 1.68042 and m of 0.0198 for a constant n of 0.4 for heating conditions where straight heat exchanger pipe heating large pool have ranges of $2554 \leq Re \leq 10640$ and $0.00434 \leq Pr \leq 0.00291$. The relationship between the Nusselt number with the Reynold number and Prandtl number in this experiment shows that comparison with other researchers' correlation does not fit with the average deviation ±77 % that occurs from the cooling process in the large pool that affected a dominated heat transfer behavior by the capacity of absorption from water inside water cooling tank.

ACKNOWLEDGMENTS

Research Grant that funded this research was from *Riset Inovasi untuk Indonesia Maju* (RIIM) batch 1 the year 2022-2025 with contract number B-811/II.7.5/FR/6/2022 and B-103/III.2/HK.04.03/ 7/2022. Thank you to the Head of Research Centre for Nuclear Reactor Technology, Research Organization for Nuclear Energy (BATAN), and National Research and Innovation Agency (BRIN). Also, special thanks to all members of Nuclear Reactor Thermal-Fluids System (RTFSys.) research group.

AUTHOR CONTRIBUTION

E. P. Ariesta, Deendarlianto and M. Juarsa are equally contributed as the main contributors to this paper. All authors read and approved the final version of the paper.

REFERENCES

1. M. Aoki and G. Rothwell, Energy Policy **53** (2013) 240.
2. P. K. Vijayan, M. H. Bade, D. Saha *et al.*, A Generalized Correlation for the Steady State Flow in Single-Phase Natural Circulation Loops, Bhabha Atomic Research Centre, Mumbai (2000) 1.
3. M. Juarsa, J. H. Purba, M. H. Kusuma *et al.*, Atom Indones. **40** (2014) 141.
4. M. Misale, P. Garibaldi, J. C. Passos *et al.*, Exp. Therm Fluid Sci. **31** (2007) 1111.
5. IAEA, Natural Circulation Data and Methods for Advanced Water Cooled Nuclear Power Plant Designs, International Atomic Energy Agency, Vienna (2002) 1.
6. E. Krepper and M. Beyer, Nucl. Eng. Des. **240** (2010) 3170.
7. A. R. Antariksawan, S. Widodo, M. Juarsa *et al.,* Atom Indones. **45** (2019) 17.
8. D. Lu, Y. Zhang, X. Fu *et al.,* Ann. Nucl. Energy **98** (2016) 226.
9. K. Il Ahn, Y. H. Jung, J. U. Shin *et al.*, Ann. Nucl. Energy **113** (2018) 353.
10. T. Yonomoto, Y. Kukita and R. R. Schultz, Nucl. Technol. **124** (1998) 18.

11. N. M. Ahmed, P. Gao and S. Bello, IOP Conf. Ser.: Earth Environ. Sci. **467** (2020) 012077.
12. Y. Zhang, Y. Yuan, L. Feng *et al.*, Appl. Therm. Eng. **159** (2019) 113876.
13. M. Gui, Q. Bi, G. Zhu *et al.*, Nucl. Eng. Des. **346** (2019) 220.
14. Y. Zhang, Q. Yu, X. Zhang *et al.*, Prog. Nucl. Energy **151** (2022) 104331.
15. W. C. Williams, Int. J. Heat Mass Transfer **54** (2011) 1682.
16. Harmen, W. Adriansyah, Abdurrachim *et al.*, AIP Conf. Proc. **1984** (2018) 020011-1.
17. R. M. Young and E. Pfender, Plasma Chem. Plasma Process. **7** (1987) 211.
18. W. Chen, X. Fang, Y. Xu *et al.*, Ann. Nucl. Energy **76** (2015) 451.
19. M. Dostál, K. Petera and S. Solnař, EPJ Web Conf. **269** (2022) 01009.
20. Y. Zhang, D. Lu, Z. Du *et al.*, Ann. Nucl. Energy **83** (2015) 147.
21. S. M. Ammar and C. W. Park, Int. Commun. Heat Mass Transfer **118** (2020) 104819.
22. B. S. Petukhov, Adv. Heat Transfer **6** (1970) 503.
23. K. H. Kang and S. H. Chang, Int. J. Heat Mass Transfer **52** (2009) 4946.
24. F. W. Dittus and L. M. K. Boelter, Int. Commun. Heat Mass Transfer **12** (1985) 3.
25. M. Juarsa, A. R. Antariksawan, S. Widodo *et al.*, AIP Conf. Proc. **2001** (2018) 050005-1.
26. A. Rosidi, M. Juarsa, D. Haryanto *et al.*, POROS **16** (2018) 7.
27. M. Juarsa, J. P. Witoko, Giarno *et al.*, Atom Indones. **44** (2018) 123.
28. X. Wang, C. Shen, L. Liu *et al.*, Ann. Nucl. Energy **181** (2023) 109542.
29. M. Juarsa, A. R. Antariksawan, M. H. Kusuma *et al.*, IOP Conf. Ser.: Earth Environ. Sci. **105** (2018) 012091-1.
30. A. A. Shevaladze, P. H. Setiawan, Giarno *et al.*, Indones. J. Nucl. Sci. Technol. **23** (2022) 14.
31. H. Cheng, H. Lei and C. Dai, Energy Procedia **142** (2017) 3926.
32. V. Uruba, AIP Conf. Proc. **2118** (2019) 020003-1.
33. R. Tian, X. Dai, D. Wang *et al.*, J. Therm. Sci. **27** (2018) 213.
34. R. H. S. Winterton, Int. J. Heat Mass Transfer **41** (1997) 809.